

## Experimental studies of spin reorientations in $\text{Er}_{2-x}\text{Th}_x\text{Fe}_{14}\text{B}$

This content has been downloaded from IOPscience. Please scroll down to see the full text.

2005 J. Phys.: Condens. Matter 17 6999

(<http://iopscience.iop.org/0953-8984/17/43/017>)

View [the table of contents for this issue](#), or go to the [journal homepage](#) for more

Download details:

IP Address: 149.156.90.131

This content was downloaded on 17/07/2014 at 14:37

Please note that [terms and conditions apply](#).

# Experimental studies of spin reorientations in $\text{Er}_{2-x}\text{Th}_x\text{Fe}_{14}\text{B}$

A T Pędziwiatr<sup>1</sup>, A Wojciechowska, B F Bogacz and S Wróbel

M Smoluchowski Institute of Physics, Jagiellonian University, Reymonta 4, 30-059 Kraków, Poland

E-mail: [ufpedziw@if.uj.edu.pl](mailto:ufpedziw@if.uj.edu.pl)

Received 21 July 2005, in final form 6 September 2005

Published 14 October 2005

Online at [stacks.iop.org/JPhysCM/17/6999](http://stacks.iop.org/JPhysCM/17/6999)

## Abstract

$\text{Er}_{2-x}\text{Th}_x\text{Fe}_{14}\text{B}$  ( $x = 0.0, 0.5, 1.0, 1.5, 2.0$ ) polycrystalline compounds have been studied with  $^{57}\text{Fe}$  Mössbauer spectroscopy, differential scanning calorimetry (DSC), magnetic measurements and x-ray diffraction. Special emphasis was put on the spin reorientation phenomena (change of spin orientation from planar to axial arrangement) occurring in this series when increasing temperature. The spin reorientation in each compound has been investigated mainly by narrow step temperature scanning in the vicinity of the spin reorientation temperature,  $T_{\text{SR}}$ .

Initial magnetization versus temperature measurements allowed us to establish the temperature regions of reorientations and the Curie temperatures of the compounds. The two-stage character of transitions was evidenced.

Mössbauer temperature scanning was performed with a step of 2 K in the vicinity of  $T_{\text{SR}}$ . The obtained spectra were analysed by using a procedure of simultaneous fitting and the transmission integral approach. Consistent fits were obtained;  $T_{\text{SR}}$  and the composition dependences of hyperfine interaction parameters were derived from fits for all studied compounds.

DSC studies proved that the spin reorientations were accompanied by thermal effects for composition  $x = 0.5$ . Transformation enthalpy and  $T_{\text{SR}}$  were determined from these studies and the two-stage character of the transition was confirmed.

The  $T_{\text{SR}}$  obtained with different methods were compared and the spin phase diagram for the series was constructed.

(Some figures in this article are in colour only in the electronic version)

<sup>1</sup> Author to whom any correspondence should be addressed.

## 1. Introduction

The intermetallic compounds based on  $\text{Er}_2\text{Fe}_{14}\text{B}$  have a tetragonal crystal lattice of the  $P4_2/mnm$  space group and belong to the  $\text{Nd}_2\text{Fe}_{14}\text{B}$  structure type, in which there are two non-equivalent positions of Nd ions (4f and 4g), six positions of Fe ions ( $16k_1$ ,  $16k_2$ ,  $8j_1$ ,  $8j_2$ , 4e, 4c) whereas the boron atom is located at one type of site (4g) [1]. Thorium is not a lanthanide, yet it was possible to incorporate it into Er sites of the crystal lattice of the  $\text{Nd}_2\text{Fe}_{14}\text{B}$  type [2], which made studies of this material more interesting.

From the point of view of fundamental studies, one of the most interesting properties of the Er-based 2:14:1 intermetallic compounds is the spin reorientation occurring in these compounds. In this process the direction of easy magnetization vector is changing at the reorientation temperature,  $T_{\text{SR}}$ , from planar (in the basal plane) to axial (along the  $c$ -axis) with increasing temperature. This is the result of a competition between axial and planar tendencies in Fe and Er [3, 4] sublattices. This phenomenon was studied previously by different groups for Gd, Y, Ce, Nd, Ho, Er, and Tm [5–13]. The study by single-crystal neutron diffraction on  $\text{Er}_2\text{Fe}_{14}\text{B}$  revealed that there is a change of crystal structure to orthorhombic below the spin reorientation transition [14].

The main goal of this work was to study the influence of Th substitution on the spin reorientation phenomena using  $^{57}\text{Fe}$  Mössbauer spectroscopy, DSC and magnetic measurements and to propose a consistent description of Mössbauer spectra in the whole range of temperatures. In addition, the thermal effects accompanying the transitions were studied quantitatively.

## 2. Experimental details

The samples of  $\text{Er}_{2-x}\text{Th}_x\text{Fe}_{14}\text{B}$  ( $x = 0.0, 0.5, 1.0, 1.5, 2.0$ ) were prepared by means of induction melting the stoichiometric proportions of the starting materials in a high purity argon atmosphere followed by annealing at  $900^\circ\text{C}$  for 2 weeks and then rapid cooling to room temperature.

X-ray, thermomagnetic analysis (TMA) and metallographical microscopy indicated the single-phase character of the materials. X-ray diffraction analysis was performed at room temperature on randomly oriented powdered samples with the use of Cr radiation. Lattice parameter refinement was conducted by a computer procedure based on Cohen's method. TMA was performed by recording magnetization versus temperature,  $M$  versus  $T$ , curves at low external magnetic field with the use of a Faraday-type magnetic balance. The Curie temperatures,  $T_{\text{C}}$ , were also determined from these measurements.

Mössbauer spectra of  $\text{Er}_{2-x}\text{Th}_x\text{Fe}_{14}\text{B}$  were recorded in the temperature range 50–330 K (with a 2 K step in the vicinity of  $T_{\text{SR}}$ ) using a  $^{57}\text{Co}$  (Rh) source and a computer driven constant acceleration mode spectrometer. The velocity scale was calibrated by a high purity iron foil. Isomer shifts were established with respect to the centre of gravity of the room temperature iron Mössbauer spectrum.

With the DSC method, the  $\text{Er}_{2-x}\text{Th}_x\text{Fe}_{14}\text{B}$  compounds have been investigated in the temperature range 100–320 K by differential scanning calorimeter (Pyris 1). The scanning rates were selected from 10 to  $60\text{ K min}^{-1}$  for heating and cooling cycles of measurements.

## 3. Results and discussion

The lattice constants of the  $\text{Er}_{2-x}\text{Th}_x\text{Fe}_{14}\text{B}$  series are given in table 1. A continuous increase of lattice parameters  $a$  and  $c$  is evidenced when the larger Th ion gradually replaces the Er ion in the crystal lattice.

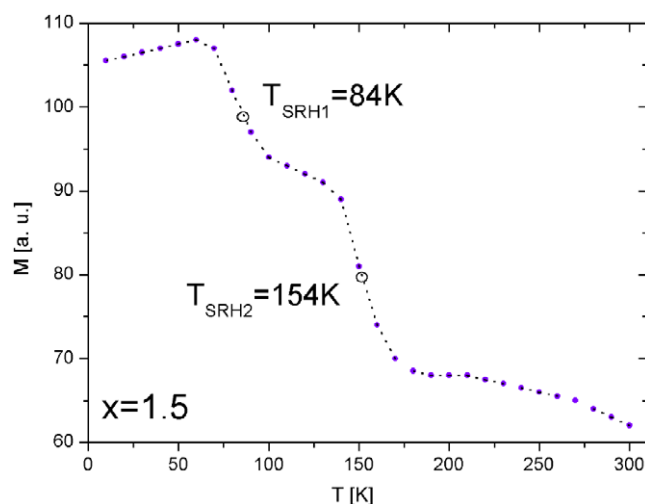


**Figure 1.** Example of irregularities on magnetization versus temperature curve evidenced in the vicinity of spin reorientations for  $\text{Er}_{2-x}\text{Th}_x\text{Fe}_{14}\text{B}$  ( $x = 1.5$ ).

**Table 1.** Lattice parameters for  $\text{Er}_{2-x}\text{Th}_x\text{Fe}_{14}\text{B}$  (room temperature).

$x$	$a$ (Å)	$c$ (Å)
0.0 [15]	8.730	11.950
0.5	8.741	11.994
1.0	8.763	12.057
1.5	8.779	12.117
2.0	8.814	12.196

The example of magnetization curves obtained at low external magnetic field of 0.8 kOe, for coarse grained materials, exhibited some anomalies in the vicinity of reorientations (see figure 1) which enabled the estimation of temperature ranges of the transitions and the approximate determination of the spin reorientation temperatures,  $T_{\text{SRH}1,2}$ . They were taken as inflection points of the descending portion of curve, following the procedure described in [16].

Very interestingly, the curves show the presence of two anomalies in the magnetization at temperatures  $T_{\text{SRH}1}$  and  $T_{\text{SRH}2}$ , respectively. The existence of two humps on the  $M$  versus  $T$  curve (figure 1) suggests a two-stage transition. The rise in  $M(T)$  in the range 5–70 K is an experimental artefact due to misalignment of virgin coarse grains (the sample was not exposed to any magnetic field before the measurement).

The values of  $T_{\text{SRH}}$  are listed in table 2, showing a gradual decrease with increasing Th content. The Curie temperatures obtained for the series are also listed in table 2. They differ by 78 K between the end members of the series.

A large number of  $^{57}\text{Fe}$  Mössbauer effect spectra for the  $\text{Er}_{2-x}\text{Th}_x\text{Fe}_{14}\text{B}$  was measured in the regions below, above and during the transitions. The Mössbauer spectra were analysed with a transmission integral approach [17]. Each subspectrum was characterized by the three hyperfine interaction parameters: isomer shift—IS, hyperfine magnetic field— $B$ , and quadrupole splitting—QS (defined as  $[(V_6 - V_5) - (V_2 - V_1)]2^{-1}$ , where  $V_i$  are velocities corresponding to Mössbauer line positions). One common set of three line widths was used for all Zeeman subspectra. A procedure of simultaneous fitting of several spectra

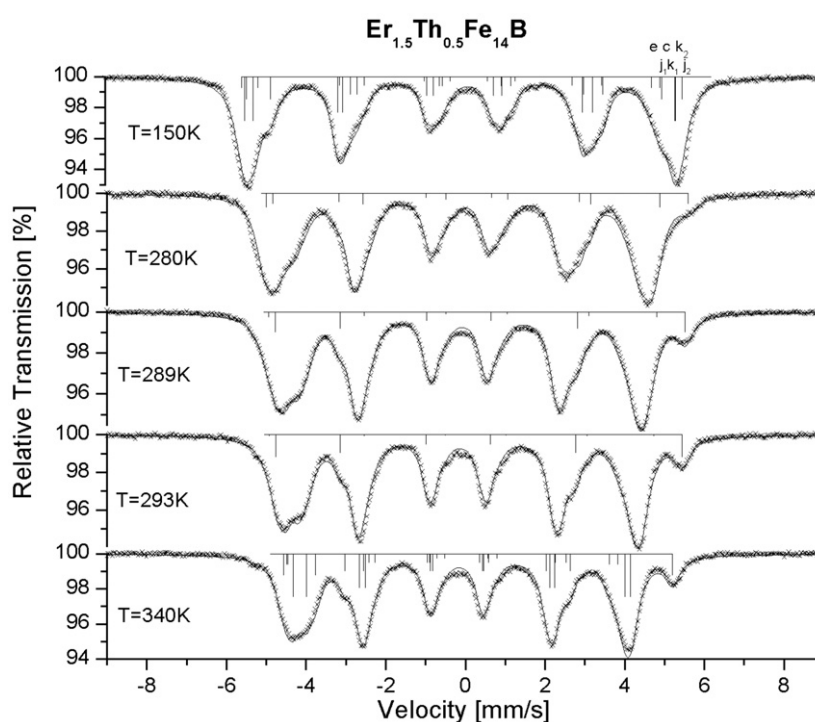


**Figure 2.** The selected experimental  $^{57}\text{Fe}$  Mössbauer spectra of  $\text{Er}_{2-x}\text{Th}_x\text{Fe}_{14}\text{B}$ ,  $x = 0.5$  intermetallic compound. The solid lines are fits to the data. The stick diagrams show the line positions and their relative intensities. Inside the region of spin reorientation, for clarity of presentation, only the positions of lines of the  $8j_2$  sublattice are marked.

**Table 2.** Values of the spin reorientation temperatures for  $\text{Er}_{2-x}\text{Th}_x\text{Fe}_{14}\text{B}$ :  $T_{\text{SRH1,2}}$ —from magnetic measurements;  $T_{\text{SRM1,2}}$ —from Mössbauer studies;  $T_{\text{SRC1,2}}$ —from DSC;  $T_{\text{C}}$ —Curie temperature;  $\Delta H$ —transformation enthalpy.  $T_{\text{SRH}}$  error is  $\pm 2$  K;  $T_{\text{SRM}}$  and  $T_{\text{SRC}}$  error is  $\pm 1$  K;  $\Delta H$  error is  $\pm 0.03$  J  $\text{g}^{-1}$ .

$x$	$T_{\text{SRH1}}$ (K)	$T_{\text{SRH2}}$ (K)	$T_{\text{SRM1}}$ (K)	$T_{\text{SRM2}}$ (K)	$T_{\text{SRC1}}$ (K)	$T_{\text{SRC2}}$ (K)	$T_{\text{C}}$ (K)	$\Delta H$ (J $\text{g}^{-1}$ )
0.0	325	325	324	324	326	326	559	0.32
0.5	278	278	281	281	290	300	540	0.14
1.0	180	235	195	246	—	—	526	—
1.5	84	154	86	145	—	—	510	—
2.0	—	—	—	—	—	—	481	—

with interconnected parameters was applied in order to get a consistent description of spectra throughout the series, similarly as in our previous studies [13, 18, 19]. Exemplary spectra are presented in figure 2. The spectrum at the top of the figure was recorded at a temperature far below the spin reorientation, whereas the bottom one was obtained far above the transition process; the three intermediate spectra were measured at temperatures inside the spin reorientation region. The spectra below and above the temperature region of spin reorientation were described using six Zeeman subspectra, called ‘low’ and ‘high temperature’ Zeeman subspectra, respectively, with relative intensities according to iron occupation of the crystallographic sublattices (4:4:2:2:1:1). Inside the temperature region of spin transition a

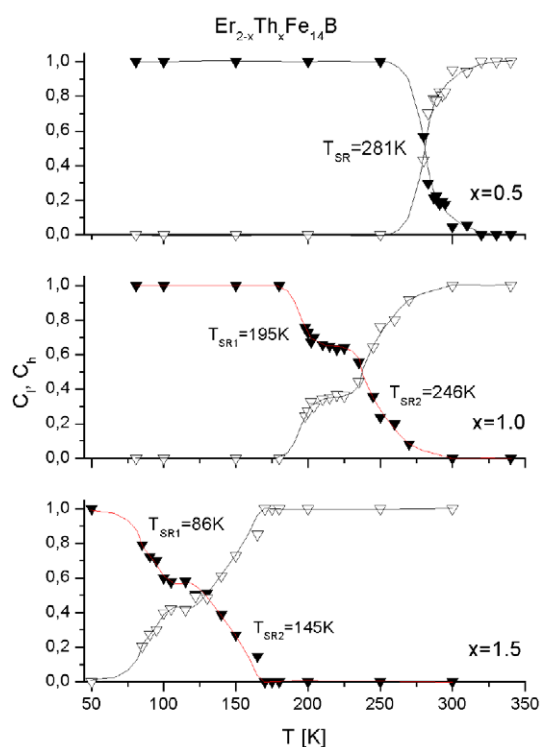


**Figure 3.** The temperature dependences of subspectra contributions for  $C_l$ —‘low temperature’ (solid triangle)—and  $C_h$ —‘high temperature’ (open triangle)—Zeeman sextets for  $\text{Er}_{2-x}\text{Th}_x\text{Fe}_{14}\text{B}$ .

coexistence of the ‘low’ and the ‘high temperature’ Zeeman subspectra was assumed, which in consequence gave 12 Zeeman sextets in the spectrum. This assumption was chosen as giving best results out of many attempts at fitting the spectra using different configurations of Zeeman subspectra and is supported by the analysis of fitting procedure for similar (Y- and Ce-substituted) compounds [13, 19]. In the course of transition, these ‘low’ and ‘high temperature’ Zeeman sextets exchange gradually (between themselves) their contributions  $C_l$ ,  $C_h$  to the total spectrum ( $C_l + C_h = 1$ ,  $C_l$  and  $C_h$  were assumed to be equal for all subspectra). The clear separation of the sixth line of sublattice  $8j_2$  in the ‘high temperature’ spectra (see figure 2) makes it easier to estimate those contributions and to determine the spin reorientation temperatures from Mössbauer studies,  $T_{\text{SRM}}$ .

The temperature dependence of the contributions ( $C_l$ ,  $C_h$ ) of both ‘low’ and ‘high temperature’ Zeeman sextets for  $\text{Er}_{2-x}\text{Th}_x\text{Fe}_{14}\text{B}$  ( $x = 1.0, 1.5$ ) compounds (shown in figure 3) also reflects a two-stage character of the transitions. From this plot the  $T_{\text{SR1,2}}$  (the temperature corresponding to reorientation of half the number of spins on a given stage of reorientation) was derived. It was found that the substitution of Th for Er causes the decrease of the spin reorientation temperature and the reduction of planar anisotropy range.

A common linear temperature dependence of IS caused by the second order Doppler shift effect was assumed for ‘low’ and ‘high temperature’ Zeeman sextets. The systematic changes with temperature of QS (linear) and  $B$  (square polynomial) were taken into account. Also the possibility of a shift of these dependences between ‘low’ and ‘high temperature’ Zeeman

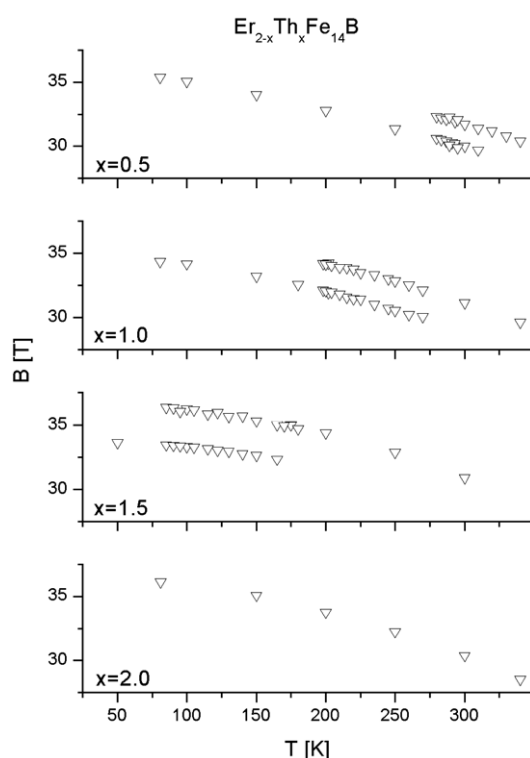


**Figure 4.** The temperature dependences of the hyperfine field,  $B$ , for  $8j_2$  crystal sites of  $\text{Er}_{2-x}\text{Th}_x\text{Fe}_{14}\text{B}$ . The average error is 0.1 T.

sextets was assumed. Figure 4 shows the temperature dependences of the hyperfine fields for  $8j_2$  sublattice of the  $\text{Er}_{2-x}\text{Th}_x\text{Fe}_{14}\text{B}$  system. In order to present clearly the behaviour of  $B$  in the reorientation region, the values for one only sublattice are shown. The value of  $B$  for subspectrum  $8j_2$  is the largest because this sublattice has the largest number of Fe ions in its nearest vicinity [20]. For all sublattices the hyperfine field decreases with the increase in temperature. A splitting of each Zeeman subspectrum into two components in the region of transition is visible.

The behaviour of QS is connected with the change of angle between the easy axis of magnetization and the electric field gradient [21]. The temperature behaviour of QS for the  $8j_2$  sublattice is shown in figure 5. For the quadrupole splitting the temperature dependence is very weak, but the values of QS are different for ‘high’ and ‘low temperature’ sextets.

In the DSC calorimetry studies the endo- and exothermic curves were observed only for the  $\text{Er}_{1.5}\text{Th}_{0.5}\text{Fe}_{14}\text{B}$  compound (presented in figure 6). For other compositions no conclusive results were obtained (the signal was too weak, the maxima were spread out). This method also confirmed that the spin reorientation phenomenon is a two-stage process. The endothermic peaks correspond to the transition from basal to axial easy magnetization direction on increasing temperature. The difference between positions of peaks for cooling and heating processes is connected with properties of the applied method and the necessity of using a large mass of sample. The spin reorientation temperatures derived from this method,  $T_{\text{SRC}}$ , were taken as the arithmetic average of temperatures obtained for heating and cooling cycles. The values of the spin reorientation temperatures determined from DSC measurements are given in table 2.

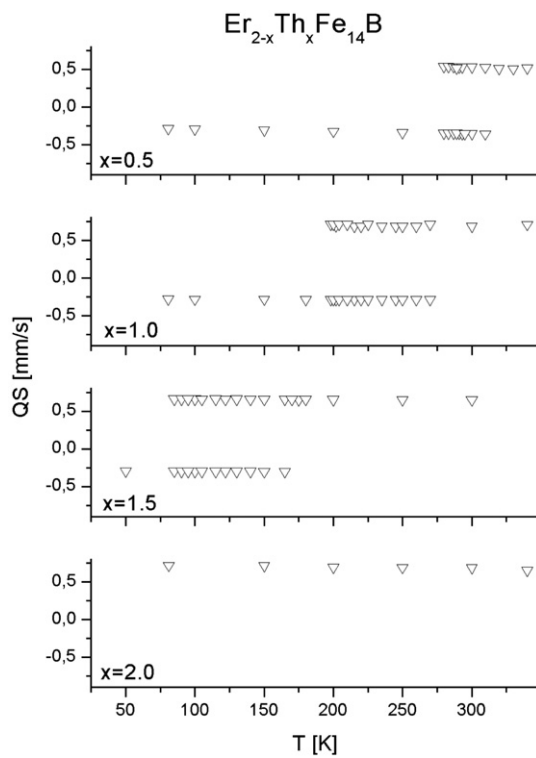


**Figure 5.** The temperature dependences of the quadrupole splitting, QS, for  $8j_2$  crystal sites of the  $\text{Er}_{2-x}\text{Th}_x\text{Fe}_{14}\text{B}$ . The average error is  $0.01 \text{ mm s}^{-1}$ .

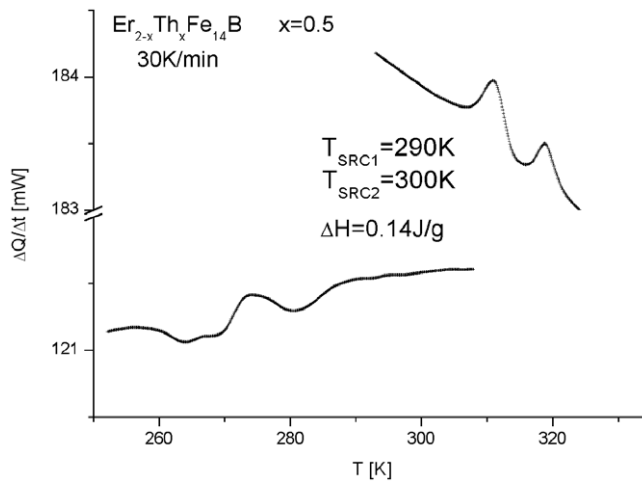


**Figure 6.** Endo- and exothermic transitions due to the spin reorientations measured with DSC for the  $\text{Er}_{1.5}\text{Th}_{0.5}\text{Fe}_{14}\text{B}$  system.  $T_{\text{SRC}1,2}$  were taken as an arithmetic average of peak positions for heating (upper curves) and cooling (lower curves) cycles.

The area under the DSC peak is defined as the transformation enthalpy,  $\Delta H$ . It was obtained as the arithmetic average of enthalpies for the cooling and heating cycles (table 2).

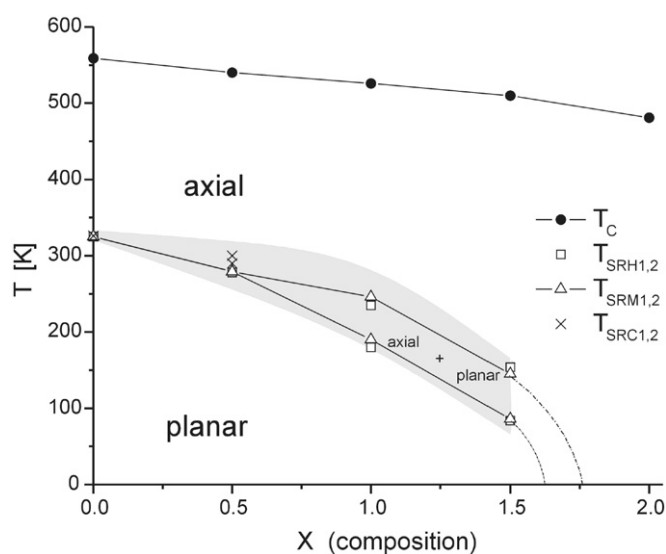


**Figure 7.** Spin structure phase diagram for the  $\text{Er}_{2-x}\text{Th}_x\text{Fe}_{14}\text{B}$  compounds.  $T_C$ —Curie temperature;  $T_{\text{SRC}1,2}$ ,  $T_{\text{SRM}1,2}$ ,  $T_{\text{SRH}1,2}$ —spin reorientation temperatures determined from DSC, Mössbauer and magnetic measurements, respectively. Dotted line—hypothetical line to guide the eye (the theoretical calculations for similar compounds [22] indicate that the lines should have a downward curvature). The shaded area marks the coexistence of axial and planar arrangements.

Figure 7 shows the magnetic phase diagram for the studied system. It is visible that the increasing content of thorium results in a decrease of the value of the spin reorientation temperature and—as a consequence—the range of axial anisotropy becomes larger. For each composition, the axial spin arrangement dominates at high temperatures while planar arrangement is present at lower temperature. The values of spin reorientation temperatures obtained with different methods (Mössbauer spectroscopy, differential scanning calorimetry and magnetic measurements) show a good agreement for all compounds studied. The two-stage process is evidenced for compounds with  $x = 0.5$  (DSC method) and for compounds with  $x > 0.5$  (magnetic measurements and Mössbauer spectroscopy). The region of coexistence of axial and planar arrangements which results from Mössbauer measurements is marked by the shaded area in figure 7. The concept of conical arrangements of spins in the shaded region [22] was not confirmed by Mössbauer results.

## References

- [1] Herbst J F, Croat J J, Pinkerton F E and Yelon W B 1984 *Phys. Rev. B* **29** 4176–8
- [2] Buschow K H J, Van Noort H M and De Mooij D B 1985 *J. Less-Common Met.* **109** 79
- [3] Givord D, Li H S and Perrier de la Bâthie R 1984 *Solid State Commun.* **51** 857–60
- [4] Hirosawa S, Matsuura Y, Yamamoto H, Fujimura S, Sagawa M and Yamauchi H 1986 *J. Appl. Phys.* **59** 873–9
- [5] Burzo E 1998 *Rep. Prog. Phys.* **61** 1099–266
- [6] Buschow K H J 1988 *Ferromagnetic Materials* vol 4, ed E P Wohlfarth and K H J Buschow (Amsterdam: Elsevier) pp 1–129
- [7] Buschow K H J 1991 *Rep. Prog. Phys.* **54** 1123–213
- [8] Ibarra M R, Arnold Z, Algarabel P A, Morellon L and Kamarad J 1992 *J. Phys.: Condens. Matter* **4** 9721–34
- [9] Pędziwiatr A T and Wallace W E 1986 *J. Less-Common Met.* **126** 41–51
- [10] Piqué C, Burriel R and Bartolomé J 1996 *J. Magn. Magn. Mater.* **154** 71–82
- [11] Koon N C, Das B N and Williams C M 1986 *J. Magn. Magn. Mater.* **54–57** 523

- [12] Wielgosz R, Pędziwiatr A T, Bogacz B F and Wróbel S 2000 *Mol. Phys. Rep.* **30** 167–73
- [13] Pędziwiatr A T, Bogacz B F, Wojciechowska A and Wróbel S 2005 *J. Alloys Compounds* **396** 54–8
- [14] Wolfers P, Bacmann M and Fruchart D 2001 *J. Alloys Compounds* **317/318** 39–43
- [15] Herbst J F 1991 *Rev. Mod. Phys.* **63** 819–98
- [16] Boltich E B, Pędziwiatr A T and Wallace W E 1987 *J. Magn. Magn. Mater.* **66** 317–22
- [17] Bogacz B F 2000 *Mol. Phys. Rep.* **30** 15–20
- [18] Wielgosz R, Pędziwiatr A T, Bogacz B F and Wróbel S 2000 *Mol. Phys. Rep.* **30** 167–73
- [19] Pędziwiatr A T, Bogacz B F and Gargula R 2002 *J. Magn. Magn. Mater.* **248** 19–25
- [20] Long G J and Grandjean F 1990 *Supermagnets—Hard Magnetic Materials (NATO ASI Series)* (Dordrecht: Kluwer) p 261
- [21] Gütlich P, Link R and Trautwein A 1978 *Mössbauer Spectroscopy and Transition Metal Chemistry* (Berlin: Springer)
- [22] Pędziwiatr A T, Bogacz B F and Gargula R 2003 *Nukleonika* **48** (Suppl. 1) 59